Observation and Modeling of Filtering Penalties in Optical Switched Networks

(Article begins on next page)

22 December 2024

Observation and Modeling of Filtering Penalties
in Optical Switched Networks

Emanuele Virgillito[1], Stefano Straullu[2], Andrea Castoldi[3], Fransisco M. Rodriguez[3], Rosanna Pastorelli[3], Vittorio Curri[1]

[1]*DET, Politecnico di Torino, Torino, Italy, emanuele.virgillito@polito.it*
[2]*LINKS Foundation, Torino, Italy, stefano.straullu@linksfoundation.com*
[3]*SM-Optics, Cologno Monzese, Italy, andrea.castoldi@sm-optics.com*

Abstract: Flex-grid WSS filters in ROADMs can degrade signal quality of transmission (QoT) due to single-sided (SS) and dual-sided (DS) passband narrowing from frequency deviations or multi-carrier transceivers. Moreover, filtering QoT penalty depends on the relative placement of ASE and filters and on the implementation-dependent capabilities of the DSP receiver. We first validate an already published model based on time-consuming experimental calibration on commercial devices including SS filter response. We then present and validate using numerical simulations a faster analytical approach based on the MMSE theory suitable for modern networks digital twins and planners. © 2024 The Author(s)

1. Introduction

The standardization of coherent technology through digital signal processing (DSP) transceivers (TRX) as open pluggable interfaces and the implementation of software-defined networking [1] necessitates a lighpath computation engine (L-PCE). In core networks, lightpaths can be accurately modeled using the generalized signal-to-noise ratio (GSNR) by considering the effects of amplified spontaneous emission (ASE) noise, non-linear interference (NLI) [2] and the transceiver noise [7]. However, less focus has been placed on the optical routing issues, especially on the filtering effects introduced by the wavelength selective switches (WSS)s in reconfigurable optical add-drop multiplexers (ROADM). Metropolitan meshed networks, which often involve several switching sites along the lightpath and experience less ASE noise due to shorter distances, must account for the quality of transmission (QoT) degradation caused by the progressive signal's spectral narrowing of the cascaded WSS filters' transfer functions [6]. This has predominantly been studied in the context of double-sided (DS) filtering, where the optical channel under test (CuT) is evenly filtered on both sides of its spectrum, a common phenomenon in the fixed-grid era [5,8,10]. However, as depicted in Fig.1a, modern flex-grid optical networks employ WSS filters that can be tuned with a granularity of 6.25 GHz, allowing for the routing of optical channels with different symbol rates or larger spectral portions composed of multiple Wavelength Division Multiplexing (WDM) channels. In such scenarios, side channels in the selected spectrum may experience single-sided (SS) filtering on one side of their spectrum Fig.1b. This effect is also relevant to multi-carrier transceivers [14], which have gained traction as a means to increase transceiver data rates with more cost-effective components without increasing the symbol rate. Additionally, SS filtering can arise from the filter nominal central frequency drift caused by manufacturing variations, adding a degree of randomness to the overall cascaded effect [9]. The overall SNR degradation caused by filters has been shown to depend on the relative distribution of ASE and filters along the optical link [3–6,9].
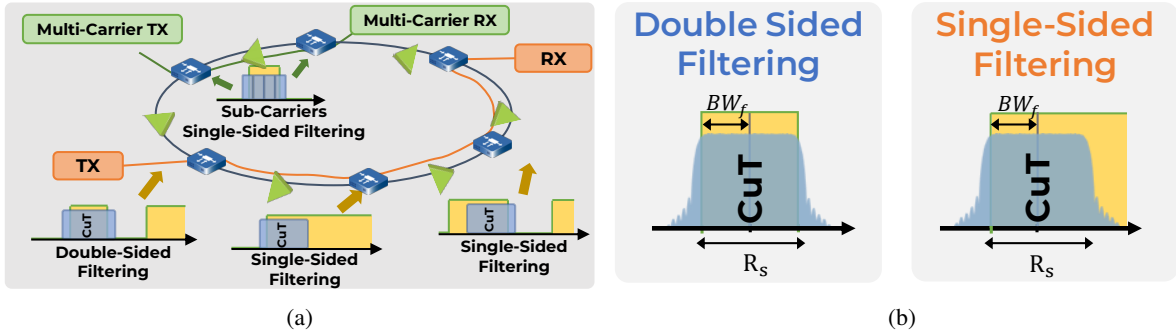

Fig. 1: (a) Representation of the flex-grid use-case that can make DS and SS filtering significant for a network channel. (b) DS and SS filter characteristics and definition of filter bandwidth BW_f

Moreover, it is heavily dependent on the DSP implementation through the adaptive equalizer's capability to recover the intersymbol interference (ISI) induced by channel's high-frequency components trimming. Hence, a reliable filtering QoT estimation based on a generic, conservative model or preliminary transceiver characterization, is critical during network planning and within the L-PCE for network configuration. (Semi)-analytical models have been proposed in literature [3–5, 15]. Those based on transceiver calibration are able to precisely include implementation dependent effects, but require time-consuming experimental characterization. Furthermore, most of them have focused on the DS filter response, with fewer efforts addressing SS filtering [13] with respect to ASE noise placement and, to our knowledge, they do not provide a sufficiently general theoretical background. In this paper, we carry out an experimental campaign comparing DS and SS filtering on a single-carrier optical channel generated by a commercial 400G transceiver. We demonstrate that DS filtering results in higher QoT penalties compared to SS and that the both are well modeled by the transceiver calibration approach of [3]. We also present and validate with numerical simulations the first step towards a generic semi-analytical model for filtering penalty estimation based on the minimum mean square error (MMSE) which does not require or limits experimental characterizations.

2. Experimental activities

The system block scheme in presence of filtering is reported in Fig.2a. At the receiver input, the QoT is measured using the generalized SNR (GSNR), which includes all the additive noise sources:

$$\text{GSNR}^{-1} = \text{SNR}_{\text{TRX}}^{-1} + \text{SNR}_{\text{ASE}}^{-1} + \text{SNR}_{\text{NLI}}^{-1} \tag{1}$$

Where SNR_{TRX} is the inherent transceiver noise, $\text{SNR}_{\text{ASE}} = \text{OSNR} \cdot \frac{B_n}{R_s}$ is the ASE noise contribution converted in the symbol rate R_s noise bandwidth and SNR_{NLI} is due to the Kerr effect, here neglected as we do not include substantial fiber propagation throughout this paper. The final BER performance however depend on the SNR, i.e. that one obtained on the received constellation samples after the DSP, through the theoretical formula $\text{BER} = k_1 \cdot \text{erfc}(k_2\sqrt{\text{SNR}})$, being $k_{1,2}$ constants depending on the modulation format. In absence of filters, the channel is AWGN and $\text{SNR} \approx \text{GSNR}$. Filters cascade introduces ISI by attenuating CuT's high frequency components. The DSP adaptive equalizer estimates the channel response and implements a MMSE equalizer minimizing the distance between the transmitted and received symbols [17], thus balancing between ISI compensation and the enhancement of the GSNR noise components. The best-case scenario occurs when all ASE is added before the filter cascade (Pre-ASE), while the worst-case occurs when ASE is moved after filtering (Post-ASE) as it is enhanced by the equalizer response trying to recover filtering [17]. Realistic configurations with distributed noise in between filters provide penalties in between these extremes [4, 12]. In this case $\text{SNR} = \Phi(\text{GSNR})$, being $\Phi(\cdot)$ a non-linear function which is also dependent on practical receiver implementation [3, 16]. Hence, the problem is to estimate the GSNR-SNR relationship to correctly estimate the BER using the theoretical formula.
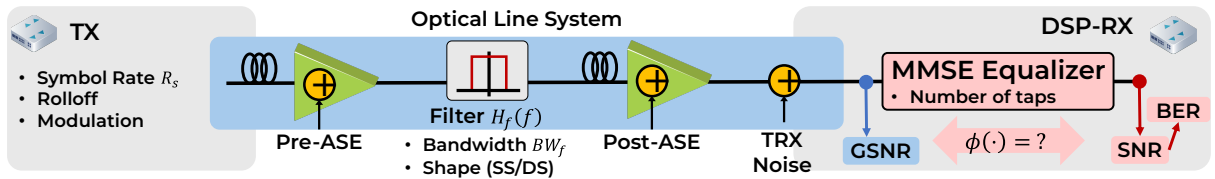
(a) System block diagram of an optical link in presence of filtering. Equalizer implements MMSE.
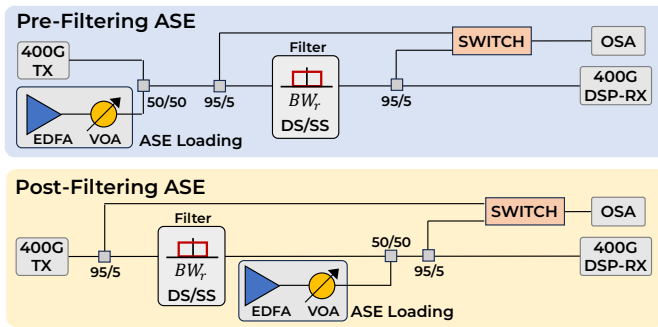
(b)
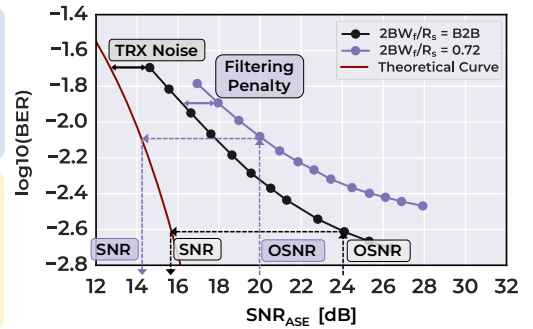
(c)

Fig. 2: (b) Experimental setup for ASE loading placed all before (top) and all after (bottom) the filter cascade. (c) Sample BER vs curves for the SS/Pre-ASE scenario. $\text{SNR}_{\text{ASE}} = \text{OSNR} \cdot \frac{B_n}{R_s}$ is the OSNR in the symbol rate noise bandwidth
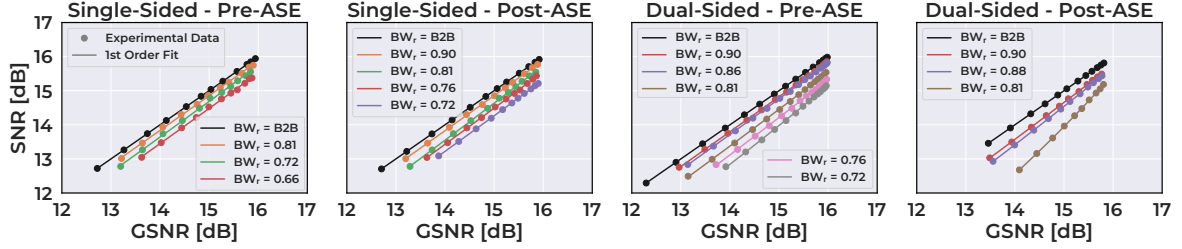
Fig. 3: GSNR vs post-equalizer SNR vs BW_r for SS (1,2) and DS (3,4) filters in Pre-ASE (1,3) and Post-ASE (2,4)) config-
urations. Circles: measured and interpolated values. Cont. lines: 1st order fit. All plots share the same y-axis scale.

We have built the experimental setup depicted in Fig.2b to observe the Pre/Post-ASE and SS/DS filtering effects
on a commercial TRX delivering 400 Gbps using DP-16-QAM at a symbol rate $R_s = 62.5$ GBaud. An EDFA in
constant power mode followed by a variable optical attenuator (VOA) is used to achieve the desired OSNR,
which is progressively varied to obtain the BER vs. SNR_{ASE} curves under various configurations. The BER is
read from the TRX DSP interface, while the OSNR is measured with an optical spectrum analyzer (OSA) on
a $B_n = 12.5$ GHz noise bandwidth. For the double-sided (DS) case, a programmable filter is used to emulate
progressive passband narrowing. The single-sided (SS) case is emulated with a band-pass filter whose central
frequency is shifted w.r.t. the CuT so that only one spectrum side is filtered. To ensure a fair SS/DS comparison,
we consider the half -3 dB filter bandwidth BW_f (Fig.1b) normalized to the symbol rate R_s, i.e. $BW_r = 2BW_f/R_s$.
For each ASE and filter response (SS/DS) we also include the case $BW_r > 1$, i.e. the non-filtered BER vs SNR_{ASE}
curves, representing the back-to-back (B2B) transceiver performance curve. A subset of such BER vs OSNR
curves [16] is reported in Fig.2c. The gap between the theoretical erfc curve (red) and the B2B curve (black) is
due to the SNR_{TRX} contribution as per Eq.1. The gap between the curve in presence of filters with $BW_r = 0.72$
(purple) and the B2B (black) is due to the filtering penalty. Being the theoretical curve (red) x-axis coordinate
the SNR, for each BW_r and each SNR_{ASE}, the corresponding SNR is the theoretical curve x-axis coordinate
delivering the same BER. Then, using Eq.1 and the B2B curves, we first extrapolate the SNR_{TRX}, which summed
to the SNR_{ASE} for all the other curve in presence of filtering gives the wanted the GSNR-SNR relationship,
reported in Fig.3 [16]. For a given GSNR, set only by ASE and TRX intrinsic noise, increasing BW_r brings to
a progressive degradation of the SNR, thus the BER. Fixed BW_r, Post-ASE configuration gives larger penalty
than Pre-ASE, as expected. SS and DS filter response show similar trends, with the SS simply showing smaller
penalties. Following the approach in [3], we fit the GSNR-SNR function using a polynomial expansion up to the
order $SNR^{-1} = \Phi(GSNR) \approx \sum_{n=0}^{N} k_n GSNR^{-n} = k_0 + k_1 \cdot GSNR^{-1}$, as well shown in [16]. In Fig.3, lines are the
1st order fitted curves which well follow the experimental values (dots). Hence, experimental characterization vs
filter bandwidth and ASE placement and filter type (SS/DS) of the $k_0, 1$ accurately estimates of the SNR, thus the
BER using the erfc formula.

3. Simulation and modelling

The previous section's estimation approach relying on experimental characterization for the unknown function
estimation $\Phi(\cdot)$ is capable of accounting for all the implementation-dependent features, such as the dependency
from the equalizer length and specific algorithm or the transceiver noise. However, it requires time-consuming
laboratory activities and equipment to characterize different transceiver, two ASE placements and some sampled
filter bandwidths. We derived an analytical expression of the $\Phi(\cdot)$ function using the MMSE theory [17]:

$$\text{SNR} = \frac{\text{GSNR}}{w_0 ||h||}, \quad w_0 = \int_{-\frac{R_s}{2}}^{\frac{R_s}{2}} \frac{df}{||h|| \left(Q(e^{-j2\pi ft}) + \text{GSNR}^{-1} \right)} \tag{2}$$

where $Q(e^{-j2\pi ft})$ is related to the DTFT of the line system filter cascade, including the signal shaping filter,
while $||h||$ accounts for the optical line system loss-gain. Hence, the filtering effect is actually a multiplicative
penalty on the GSNR as w_0, although with a non-linear dependency as w_0 is a function of GSNR itself as in [3].
Realistic equalizers have a finite number of taps, which limits the ISI recovery performance, while Eq.2 refers to
the MMSE solution for an infinite length equalizer, hence, the formula leads to an optimistic penalty estimation
w.r.t. commercial devices. However, the model formula can be adapted to finite equalizers. As a first step, we test
Eq.2 effectiveness by means of numerical simulations, whose configuration is depicted in Fig.4a. We propagate a
400G channel ($R_s = 64$ GBaud using DP-16QAM) shaped with root-raised cosine (RRC) filter with 15% roll-off
through a 3x cascade of 4-th order SuperGaussian filter with bandwidth set to have a $BW_r = [0.88, 0.91, 0.94, 1]$ in
each filter. Only DS filtering has been considered with no loss of generality. Pre-ASE and Post-ASE configurations
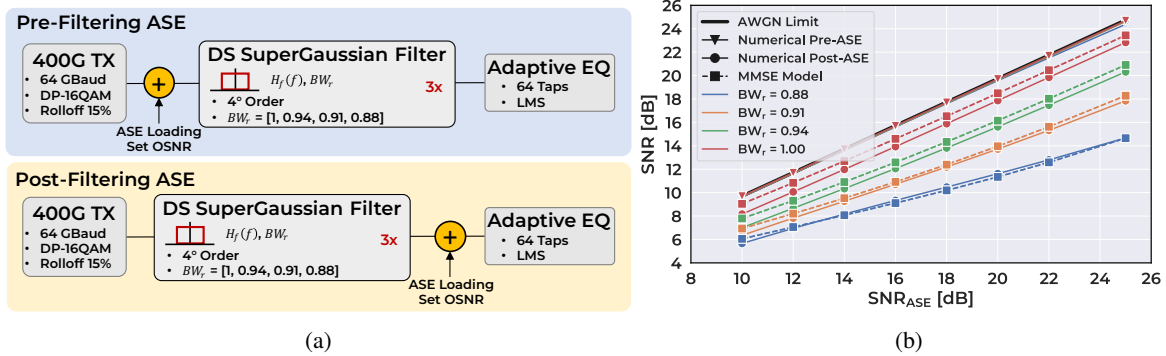
Fig. 4: (a) Simulative setup for ASE loading placed all before (top) and all after (bottom) the filter cascade. (c) SNR vs SNR_{ASE} vs BW_r: simulations (cont. curves), MMSE model (dashed curves)

have been simulated progressively increasing ASE noise loading to obtain a SNR_{ASE} between 10 and 25 dB. No transceiver noise and non-linear fiber propagation is accounted here, so that $GSNR = SNR_{ASE}$. The CuT is received using a least mean square (LMS) equalizer with 64 taps. Although real transceivers do not implement such long equalizers, this choice allows us to test the convergence to the infinite length equalizer assumption of Eq.2. For each SNR_{ASE} values, the corresponding SNR is numerically estimated on the received constellation after the equalizer. B2B simulation (no filters) have also been carried out to obtain the AWGN limit, i.e. the SNR-SNR_{ASE} relationship when the channel is AWGN. Numerical simulation results are shown in Fig.4b. The AWGN limit curve (black) shows a properly calibrated simulation, as we obtain $SNR = SNR_{ASE}$. Triangle curves show the Pre-ASE results. In Pre-ASE scenario (triangles) is jointly filtered with the signal and recovered by the equalizer, whose performance increase with its number of taps. These curves coincide with the AWGN limit for all the BW_r, verifying that the 64 taps equalizer converges to the infinite length assumption in the considered configurations. Post-ASE configurations (circles) instead show a significant penalty to the AWGN limit with tighter BW_r due to the ASE noise enhancement at the equalizer. The analytical model (dashed lines) scales well with the phenomenon trends, although they still provide slightly optimistic predictions, with no more than 1 dB of gap to the simulations. This demonstrates good premises for the generalization of the MMSE model to arbitrary line configurations, although some further development is needed to mitigate the underestimation.

4. Conclusions

We have presented the experimental validation of the transceiver calibration-based model of [3] on commercial transceiver with SS filtering response. Although this model is able to encompass the implementation-specific performance, we developed an analytical model to provide a rough estimation of the filtering impairment by knowing the line GSNR, the filters frequency response and the transceiver roll-off characterization. These results lay the foundation for a semi-analytical model decoupling the filtering degradation from the other impairments and which can be extended to distribute ASE-filters configurations for QoT estimation in the control plane of modern dynamic optical networks. Although these preliminary results accounts for optimistic infinite length equalizers, further steps will specialize to finite-length implementation as in [17]. While the former can be employed as a first, rough estimation in the network planning phase, we envision the usage of the latter jointly with a smaller set of transceiver characterization to estimate an equalizer length parameter and refine the SNR estimations.

References

1. Gharbaoui, M., et al. An Experimental Study on Latency-Aware ... . *Computer Networks*. **208** pp. 108880 (2022,5)
2. Curri, V. GNPy Model of the Physical Layer for Open and Disaggregated ... . *JOCN*. **14**, C92-C104 (2022,6)
3. Delezoide, C., et al. On the Performance Prediction of Optical Transmission... . *ICTON 2017*. pp. 1-4 (2017,7)
4. Delezoide, C., et al. Weighted Filter Penalty Prediction for QoT Estimation. *OFC 2018*. pp. 1-3 (2018,3)
5. Fernandez De Jauregui Ruiz, I., et al. An Accurate Model for System ... . *ECOC 2019*. pp. 378 (4 pp.)-378 (4 pp.) (2019)
6. Hsueh, Y., et al. Passband Narrowing and Crosstalk Impairments in ROADM-Enabled... . *JLT*. **30**, 3980-3986 (2012,12)
7. Mano, T., et al. Modeling the Input Power Dependency of Transceiver... . *OFC 2024*. pp. M1H.4 (2024,3
8. Okamura, K., et al. Pre-Filtering Techniques for Spectrum Narrowing Caused... . *IEEE Photonics J.*. **13**, 1-13 (2021,4)
9. Pal, B., Zong, et al. Statistical Method for ROADM Cascade Penalty. *OFC 2010*. pp. 1-3 (2010,3)
10. Pan, J., Pulikkaseril, et al. Comparison of ROADM Filter Shape Models for ... . *IPC 2016*. pp. 550-551 (2016,10)
11. Wang, Q., et al. Accurate Model to Predict Performance of Coherent... . *Opt.Express*. **26**, 12970-12984 (2018,5)
12. Zami, T., et al. Filter-Induced OSNR Penalty in WDM Fiber Networks ... . *OSA APC 2020* pp. NeTu1B.4 (2020,7)
13. Searcy, S., et al. Experimental Comparison of Single-Sided and Double-Sided Filtering ... . *IPC 2023*. pp. 1-2 (2023,11)
14. Lorences-Riesgo, A., et al. Maximizing Fiber Capacity in Flex-Grid ... . *IEEE PTL*. **34**, 161-164 (2022,2)
15. Torres-Ferrera P., et al. Filtering Power Penalty Evaluation of Coherent Systems ... . *ONDM 2024*.
16. Virgillito E., et al. Experimental Analysis and Modeling of Single-Sided Vs Dual-Sided Filtering ... . *ONDM 2024*.
17. Proakis, J. Digital communications. (McGraw-Hill,2008)